Journal of Geology & Geophysics
ISSN: 2381-8719

Mekkawi et al., J Geol Geophys 2017, 6:6
DOI: 10.4172/2381-8719.1000311

Research Article Open Access

Seismic Risk Zones and Faults Characterization using Geophysical Data

Mahmoud Mohamed Mekkawi*, El Sayed A Fergani and Klaled A Abdella

Department of Applied Geophysics, National Research Institute of Astronomy and Geophysics, Geomagnetism and Geoelectricity, Egypt

Abstract

Understanding and imaging the real seismo-tectonic of SW-Cairo zone are essential to eliminate the risk of this hazardous seismic zone which is surrounded by the highest condense population province in Egypt. In this study, up to date earthquake catalogue and aeromagnetic data of the area under study were analyzed for tracing active subsurface faults that are responsible of earthquakes activity. Using 2D-power spectrum techniques, depth of structures (faults) was estimated and a shallow intrusion was detected at 550 m. The tectonic framework of SW-Cairo was evaluated and discussed in view of seismicity, surface geology, subsurface structures from RTP maps and boreholes information and the active faults were traced at shallow and deep depths.

Keywords: Seismicity; Aeromagnetic data; Subsurface structures; Sctive faults; SW-Cairo

Introduction

A paramount criterion in the assessment earthquake hazard and risk analysis is imaging and understanding the seismo-tectonic structures to trace the active seismic faults in the low and moderate seismic activity regions. Identified the main active faults where the earthquakes foci take place can lead to a reliable simulation source function of expected earthquakes. This work is concerned with the south west Cairo area situated between longitudes 30.4° and 32.1° E and latitudes 28.8° and 30.0° N (Figure 1). Cairo, the capital of Egypt, is ranked as one of the most populated cities in the world. Nicknamed "The City of a Thousand Minarets" for its preponderance of Islamic architecture. The study area includes the Pyramids of Giza, one of the Seven Wonders of the World and the most famous monuments of ancient Egypt. These massive stone structures were built around 4500 years ago on a rocky desert plateau close to the Nile.

Seismically, the study area is the most dangerous seismic area in Egypt. Spatial distribution of historical and recent earthquake foci indicates that Egypt had been suffered from both interplate and intraplate events. Most earthquake activity in Egypt takes place in specific zones of Aqaba Gulf, north Red Sea, Suez Gulf, Dahsour and Aswan (Figure 1). The recent one which caused huge damage in human and his properties is the Dahshour seismic zone, where 1992 earthquake with 5.8 magnitude took place. The ratio of damage is high in relative to earthquake size which took highly attention of seismologists and engineers to understand the main causes of this huge damage accompanied to a moderate earthquake. Fergany and Sawada [1] concluded that the direct causes of damage were due to the quaternary sediment effect and the fragile buildings. The damage was concentrated in Giza, Cairo and southern provinces of Nile Delta where the Nile alluvium are common. Figure 2 draws the isoseismal intensity map of the Cairo 1992 earthquake with elongated shape with the Nile Valley extension as a result of the Nile deposits effects on the seismic waves.

The present work integrated the surface geology, deep seated drilling wells, subsurface structures features present by the RTP aeromagnetic map, deep magnetotrlluric model [2] and updating compiled seismicity catalogue to image and understanding the active seismo-tectonic structures that caused micro, small and moderate earthquakes.

Geological and Boreholes Information

The study area occupies one of the spectacular depressions in the Eocene limestone plateau of the Western Desert of Egypt. It has three main basin structures of Fayoum, Wadi Rayan and Nile valley in the Northern Western Desert. Geologically, the area extends from the southwest of Cairo to Gabal Qatrani at to east; northeast of the Qarun Lake, southwest of the Wadi Rayan and Nile valley occupy the eastern part of the study area. The geological units of the study area (Figure 3) started from Middle Eocene, to Recent Nile sediments [3]. The earliest geological studies and tectonic features of the northwestern desert were conducted by many authors [4-14].

El-Shazly [11], considered that the E-W trend is the oldest tectonic trend that affected the Egyptian basement rocks some time during Pre-Cambrian due to a northern horizontal pressure. Meshref [13] stated that the basement rocks in the Western Desert of Egypt have been affected by the oldest EW and ENE trending faults which in turn are intersected by younger NW and NNW trending faults. These two fault systems have large vertical and horizontal displacements. The area of Dahshour-Qattrani, in particular, is affected by the NW and EW trending faults. The NW trending fault, called the Qattrani fault, has a throw of about 350 m. However, the EW trending fault, called the G. Sheeb fault, has a throw between 150 and 200 m. The Oligocene basalt occupies these two faults.

Said [14], stated that the structure of the area is dominated by faults, many of which can be identified from seismic and well data. The majorities are steep normal faults and most of them have a long history of growth, and some of the normal faults suffered strike slip movements during part of their history. Strike slip movements seem to have affected the orientation of many of the old fold axes. The strike slip movements

***Corresponding author:** Mahmoud Mohamed Mekkawi, Proessor, Department of Applied Geophysics, National Research Institute of Astronomy and Geophysics, Geomagnetism and Geoelectricity, Egypt, Tel: +201000643221; +20233836327; E-mail: mekkawi05@yahoo.com

Received September 16, 2017; **Accepted** October 27, 2017; **Published** November 03, 2017

Citation: Mekkawi MM, Fergani ESA, Abdella KA (2017) Seismic Risk Zones and Faults Characterization using Geophysical Data. J Geol Geophys 6: 311. doi: 10.4172/2381-8719.1000311

Figure 1: Map of common tourist places in Egypt (Red rectangle shows the study area borders).

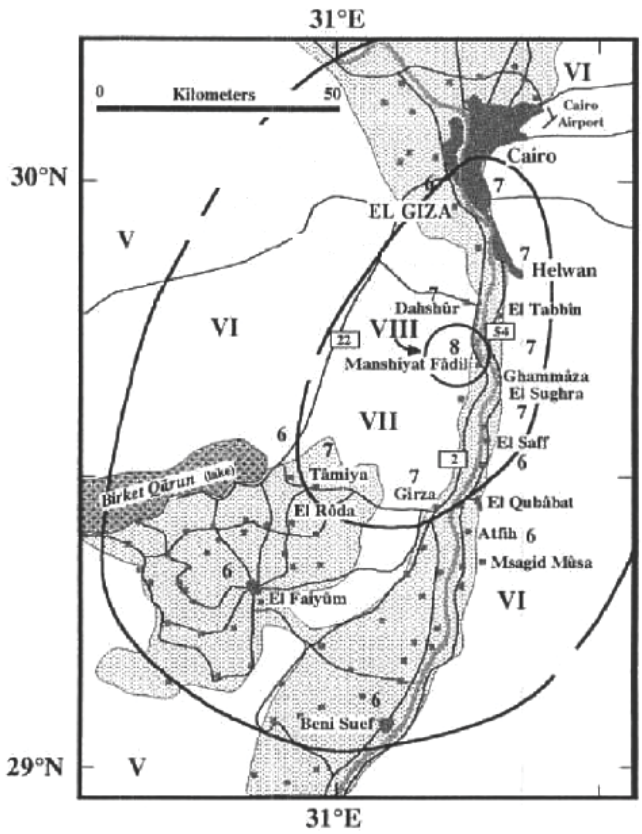

Figure 2: Modified Mercalli Intensity (MMI) distribution of October 12, 1992 earthquake (Thenhaus et al.). Grey areas represent agricultural lands while dark grey area is urban region.

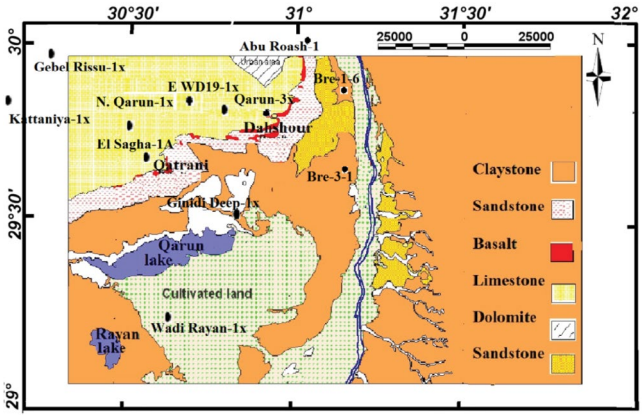

Figure 3: Geological Map of the study area (Geological survey of Egypt, 2003) with available boreholes information.

were probably related to the lateral movements which the Africa plate underwent during the Jurassic and Late Cretaceous.

It notes that, basaltic sheets covered the surface of Dahshour and Qatrani areas where the subsurface sedimentary successions, stratigraphy and structure prevailing are dominated by faults, many of which can be identified from boreholes information (Figure 4).

Seismicity Data

Although Egypt is characterized by low to moderate seismic activity, high risk was happen in the provinces of Great Cairo, highest population density in Egypt. The seismicity of Egypt has been studied by many authors [15-21].The seismo-tectonic zones and the highest seismic activity were identified along the Gulf of Aqaba–Dead Sea transform, the Northern Red Sea triple junction point, Aswan, Cairo-Suez District and Dahshur-Qatrani (SW-Cairo). Historically, Egypt threated damaged earthquakes were back from 2200 BC to 1899 (Figure 5). Most of historical earthquakes were located in the study area with intensity ranged from V to IX.

Instrumental earthquake observation has begun since 1989 with one seismic station installed in Helwan, south Cairo. The number of seismic stations increased gradually until the occurrence of 1992 earthquake, abrupt increasing in the monitoring system. National Research Institute of Astronomy and Geophysics, NRIAG, was responsible to install and deploy Egyptian Seismic Network that covered all Egypt with condensed observations in the effective seismic zones like as Dahshour and Aswan Zones. After this operating advanced monitoring system in Egypt, huge data base becomes available and the seismicity map extended to show all seismicity levels of micro to large earthquakes (Figure 5).

One of the recent destructive events in Egypt known as Cairo 1992 earthquake was occurred on October 12, 1992 in the study area with moment magnitude (Mw)=5.8. It left a huge damage where 554 persons have been killed, about 20,000 people injured and over one billion US$

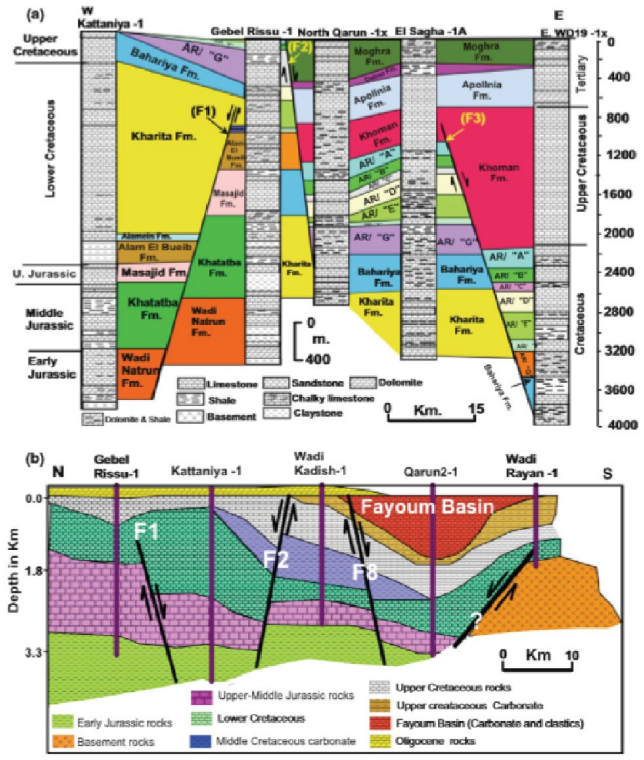

Figure 4: (**a**) Simplified structural cross section through wells Kattaniya1x, Gebel Rissu-1x, North Qarun-1x, El Sagha-1A and East WD191x along W–E direction. (**b**) Simplified structural cross section through wells Gebel Rissu-1x, Kattaniya-1x, Wadi Kadish-1, Qarun2-1 and Wadi Rayan-1 along N–S direction (After Qarun Oil Field, Internal Report, 2005).

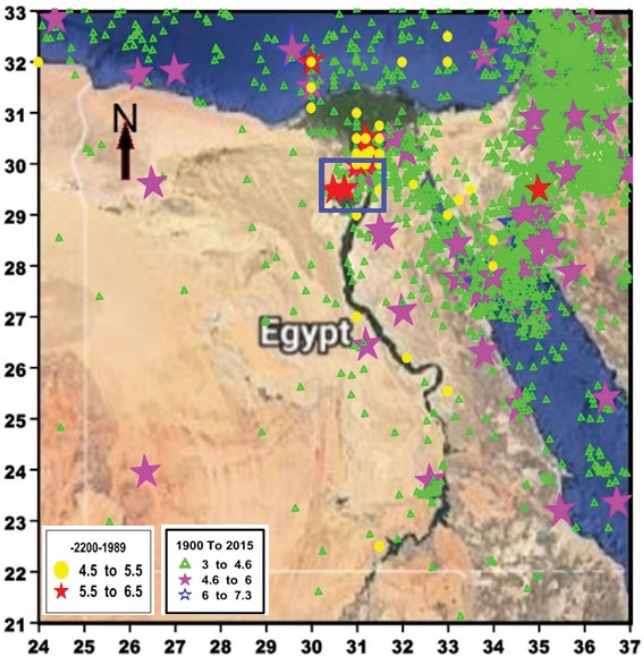

Figure 5: Seismicity map of Egypt from 2200 BC to 2015. The blue rectangle denotes the study area.

had been reported as property losses. This is not the only destructive earthquake in Egypt, but similar historical events occurred in 778, 1303 and 1847 that destroyed parts of big cities, like Cairo and Alexandria [22,23].

The seismicity of the study area increased abruptly after the occurrence of the main shock 12th October, 1992 to record a wide range of magnitude 0< M<5 located at different depths 3-30 km. Figure 6 draws an updating instrumental seismicity map of studied area from 1900 to 2015 and the fault plane solution of the main shock and some of its aftershocks. Intraplate seismicity occurs in the vicinity of stress concentrators within pre-existing zones of weakness, where the faults are intersecting. Talwani and Rajendran [24] pointed out that most intraplate earthquakes occur around the intersections of faults, and, in general, not at the intersections themselves or very close to them. The fault plane solutions indicated that the common active faults are normal faulting mechanisms with strike-slip components.

The 2D magnetotelluric inversion modelling of Mekkawiet al. was applied to transverse electric (TE), magnetic (TM) modes, and tipper (TP) data using REBOCC inversion program [25]. The 2D magnetotelluric model of (TM–TE-TP) (Figure 7). The model shows

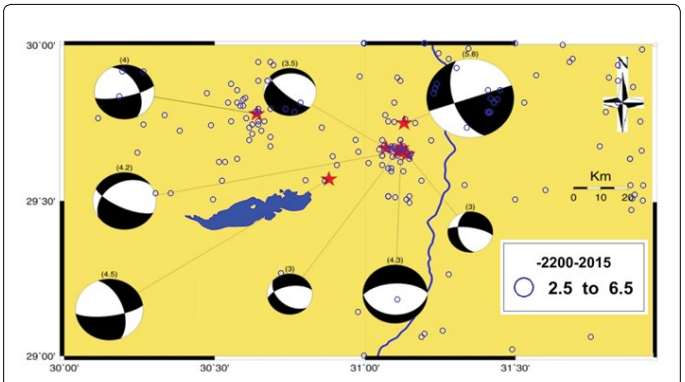

Figure 6: Seismicity of the study area (open blue circles). Focal mechanisms of Cairo 1992 earthquake and some aftershocks (red stars).

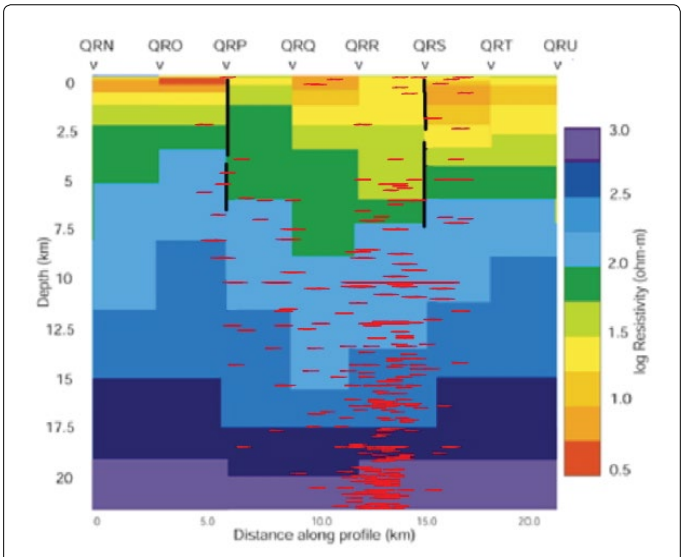

Figure 7: Final 2D-Resistivity structures based on magnetotelluric data along a Profile (QRN-QRU) crossing Fayoum-Cairo District, referring to deep basin and active faults. The symbols above the model identify the MT sites, (after Mekkawi et al.) Red symbols denote to earthquake depths along the profile.

a region of a good-conductive material located in the depth between the earth's surface and 5 km. In the central part of the model, it can be noticed the presence of high resistivity zone (could be granitic rocks). While the low resistivity part between QRQ and QRR could be due to presence of Kattaniya horst and its related ultrabasic/basic rocks. I can notice the effect of the fault structures from the changing depths along the resistivity layers. These shears are extending to about 20 km in depth. Their corresponding locations agree with the well-logging and with minor shifts due to the depths range.

Aeromagnetic Data

The reduce to the magnetic pole (RTP) aeromagnetic map (Figure 8) is characterized by high and low anomalies spreading out the map area. It displays a major trend (from NE to SW). Also, NW-SE and E-W trends are present. These magnetic trends do not occur randomly, but are aligned along definite and preferred axes that can be used to define magnetic structures. These anomalies could be related to significant susceptibility contrast between the highly magnetic volcanic rocks (basement) and the low magnetic meta-sediments. In that regards, the Geosoft program (Oasis Montaj 7.1) was used to analysis the RTP data to qualitative and quantitative to delineate both shallow and deep structures.

In the middle part, there is a large positive anomaly trending in NE-SW constituting several peaks. This anomaly reflects high magnetic susceptibility with different amplitudes. It could be due to basement structures and basic intrusions (dykes). Most of earthquakes in the area are located at the north part of this anomaly. Figures 8 and 9 show the RTP maps with seismicity catalogue at different focal depths and magnitudes. Most of earthquakes concentrate at northern part of the study areas.

Data processing and analysis

Filtering the aeromagnetic data enhances and sharpness the anomalies and trends of the data and helps in the qualitative interpretation. In order to trace the shallow structures, the analytic signal method was applied to the RTP aeromagnetic data. The amplitude of analytic signal (AAS) of the magnetic anomaly is given by equation [26]: as

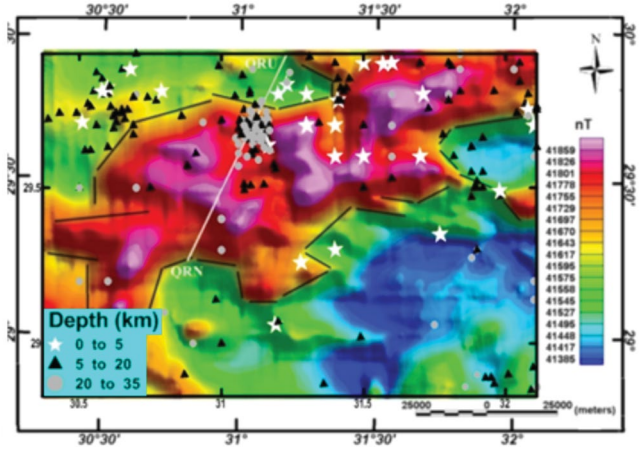

Figure 8: RTP aeromagnetic anomaly map after (after EGPC, 1990) and white line is the location of Magnetotelluric profile QRN-QRU (After Mekkawi et al.). Black lines are expected faults. All Earthquakes catalogue (1900-2015) at different focal depths).

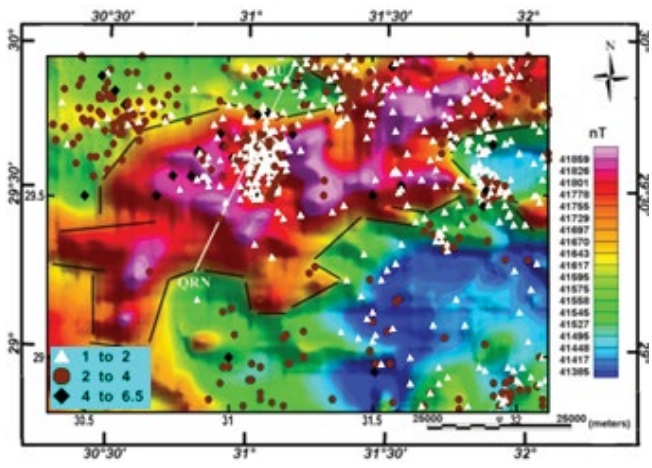

Figure 9: RTP aeromagnetic anomaly map with all Earthquakes catalogue (1900-2015) at different Magnitude.

$$AAS(x,y)=\sqrt{\left(\frac{\partial T}{\partial x}\right)^2+\left(\frac{\partial T}{\partial y}\right)^2+\left(\frac{\partial T}{\partial z}\right)^2} \quad (1)$$

The horizontal $\left(\frac{\partial T}{\partial x}+\frac{\partial T}{\partial y}\right)$ and vertical $\left(\frac{\partial T}{\partial z}\right)$ derivatives of the magnetic anomaly are Hilbert transform pairs of each other. The analytic signal method has been successfully applied to locate dike bodies. The most advantage of the analytic signal is that it has a maximum value (red contour) over the (contacts, dykes or veins). The analytical signal map is plotting with seismicity map (Figure 10). Most earthquakes of magnitude (M>4) are coincide and near to active faults.

Tilt Derivative filter (TDR) is applied to the aeromagnetic data. It is useful for mapping shallow basement structures and mineral exploration targets. This filter is estimated by dividing the vertical derivative by the total horizontal derivative Verduzco (2004) as:

$$TDR = \arctan(VDR/THDR) \quad (2)$$

$$VDR = (dT/dz) \text{ and } THDR = \text{sqrt}((dT/dx)^2 + (dT/dy)^2) \quad (3)$$

Where VDR and THDR are vertical and total horizontal derivatives, respectively of the total magnetic intensity anomaly (T). The most advantage of the TDR is that its zero contour line is on or close to the fault/contact location. Figure 11 shows the TDR angle map of the aeromagnetic data with the zero contour line (solid contour). It shows a tentative qualitative interpretation of the data and shallower structures. Generally, the area may be dissected by major faults striking in the NE-SW, NW-SE and E-W-directions. These indicate that the magnetic anomalies in the area are structurally controlled, especially for the shallower sources.

Depth estimation

The depth to the source of magnetic anomalies is valuable and important information in of subsurface structures. In order to estimate the depth of the magnetic sources, 2-D Power Spectrum methods were applied to the RTP aeromagnetic data. It is used to determine the depths of volcanic intrusions and basement complex [26,27]. In the

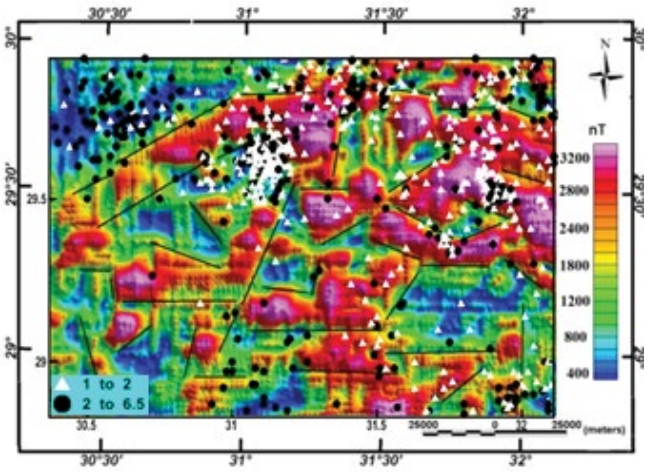

Figure 10: Analytical Signal aeromagnetic map the study area. Black lines are expected faults with seismicity map at (Mag. 1-2 and 2.1 to 6.5).

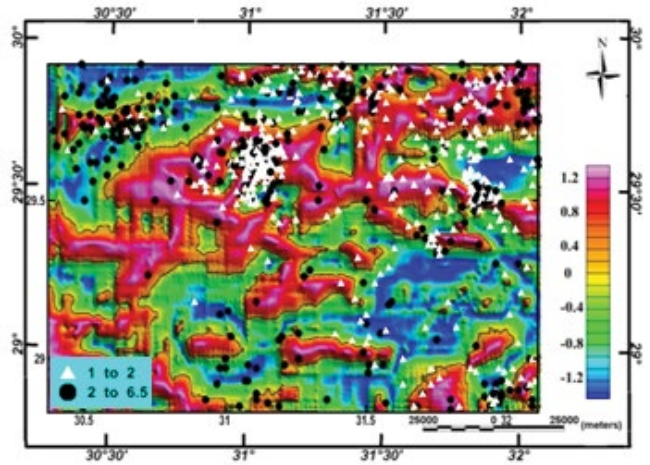

Figure 11: Tilt angle Derivative (TDR) aeromagnetic map. Solid contours are expected shallower faults or contacts with seismicity map at (Mag. 1-2 and 2.1 to 6.5).

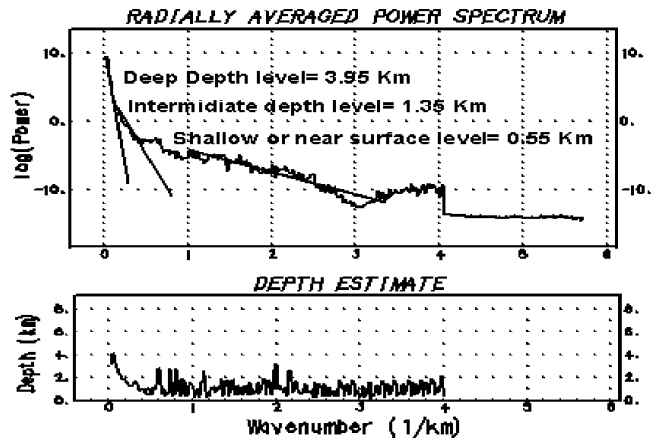

Figure 12: Radially average power spectrum and the resultant depth estimates RTP aeromagnetic map.

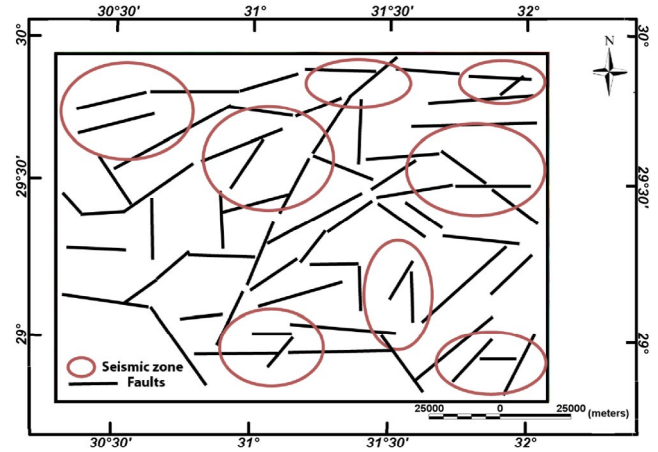

Figure 13: Black lines represent faults derived from RTP maps and red circles are seismic zones from RTP seismicity data.

present study, As a result, a two-dimensional power spectrum curve was obtained on which three main average levels (interfaces) at depth 550 m (Figure 12). (shallow intrusions) and 1350 m. (intermediate level) and 3950 m. (deep basement layer). These results are agreed with borehole information and geological cross-section [28-32].

Discussion and Conclusion

The tectonic framework of Dahshur area is illustrated by different tools (surface and subsurface) geology; boreholes information; seismicity distribution as well as magnetic data. All geophysical and geological data are integrated together to understand the tectonic and active seismic zones. Figure 7 shows Resistivity structures based on magneto telluric data along a Profile (QRN-QRU) crossing the study area, referring to deep basin more than 15 km and active faults that is responsible to the earthquakes mechanism. From RTP magnetic and seismicity data analysis, can conclude that the earthquakes distribution are concentrated in the northern parts of the study area with active seismic zones and faults (Figure 13). Also, trace the shallow and deep structures from 550 m to deep zones more than 15 km.

References

1. Fergany E, Sawada S (2009) Demonstration of pb-PSHA with Ras-Elhekma earthquake, Egypt. Seismological Research Letters 80: 5-7.
2. Mekkawi M, Khalil A, Elbohoty M, Rabeh R, Saleh S, et al. (2006) Magnetotelluric and Aeromagnetic Interpretation At Fayoum- Cairo District, Northern Western Desert, Egypt. Egyptian Geophysical Society (EGS), Geophysical Journal 1: 1-14.
3. Egyptian Geological Survey (2003) Geologic map of Dahshour– Qatrani area with scale 1:500000.
4. Zittel K (1883) Contributions to the geology and palaeontology of the Libyan desert and adjacent areas of Egypt. Palaeontographica 30: 1–112
5. Blackenhorn M (1901) News on geology and Palaontology of Egypt. III: The Miozan. Geol Ges 53: 52-132.
6. Beadnell H (1905) The topography and geology of the fayum province of Egypt. Survey Department of Egypt, Cairo, 101.
7. Caton-Thompson and Gardner (1929) Lake Moeris - Faiyum Depression - Egypt - Map 1.
8. Shata A, El-Fayomi I (1969) Remarks on the regional geological structure of

the Nile delta: Proceedings of Bucharest Symposium for hydrology of the delta. pp. 189-197.

9. Sigaeiv N (1959) The main tectonic features of Egypt. Geol Survey Egypt, Cairo.
10. Said R (1962) The geology of Egypt. Elsevier publishing Company. Amsterdam, New York.
11. El-Shazly M (1966) Structure development of Egypt. UAR, Geol Soc of Egypt, fourth Annual Meeting pp. 31-38.
12. Youssef M (1968) Structural pattern of Egypt and its interpretation. AAPG Bulletin. 52: 601-614.
13. Meshref W (1990) Tectonic framework. R. Said (Ed.) The Geology of Egypt, A.A. Balkema, Rotterdam, Netherlands pp. 113–155.
14. Said R (1990) The Geology of Egypt. Balkema Press, The Netherlands.
15. Maamoun M. Allam A, Megahed A (1984) Seismicity in Egypt. Bull HIAG pp.109-160.
16. Kebeasy R (1990) Seismicity, geology of Egypt. pp. 51–59.
17. Ambraseys N, Srbulov M (1994) Attenuation of earthquake-induced ground displacements. Earthq Eng Structural Dynamic 23: 467-487.
18. Abou Elenean K (1997) Seismotectonics of Egypt in relation to the Mediterranean and Red Seas tectonics. Ph. D. Thesis. Fac. Sc. Ain Shams Univ. pp. 200.
19. Abou Elenean K (2007) Focal mechanisms of small and moderate size earthquakes recorded by the Egyptian National Seismic Network (ENSN), Egypt. NRIAG J Geophys 6: 117–151.
20. Badawy A (1999) Historical seismicity of Egypt. Acta Geodaetica et Geophysica Hungarica. 34: 119–135.
21. Badawy A (2005) Present-day seismicity, stress field and crustal deformation of Egypt. J Seismol 9: 267–276.
22. Ambraseys N, Melville C, Adams R (1995) The seismicity of Egypt, Arabia and the Red Sea: A histircal review. Cambridge Press pp. 182.
23. El-Sayed A (1996) Seismic hazard of Egypt. Natural Hazards 10: 247-259.
24. Talwani P, Rajendran K (1991) Some Seismological and Geometric Features of Intraplate Earthquakes. Tectonophys 186: 19-41.
25. Siripunvaraporn W, Egbert G (2000) An efficient data-subspace inversion method for 2-D magnetotelluric data. Geophysics 65:791–803.
26. Roest W, Verhoef J, Pilkington M (1992) Magnetic interpretation using 3-D analytic signal. Geophysics 57: 116-125.
27. Spector A, Bhattacharya B (1966) Energy density spectrum and autocorrelation function of anomalies due to simple magnetic models. Geophys Pros 14: 242.
28. Spector A, Grant F (1970) Statistical models for interpreting aeromagnetic data. Geophysics 35: 293–302.
29. Egyptian General Petroleum Company (EGPC) (1990) RTP aeromagnetic map of the El-Fayoum area, North Western Desert, Scale 1: 100 000.
30. Naeim G, Hussein A, El-Hakim B, Sewidan A (1993) A preliminary Report on the Dahshour earthquake. Egyptian Geological Survey, Intern report, pp 1–55.
31. Shata A (1955) An introductory note on the geology of the northern period of the western desert of Egypt. Bull Desert Res Inst Egypt 5: 96–106.
32. Thenhaus P, Sharp R, Celebi M, Ibrahim A, van de Pol H, et al. (1993) Reconnaissance report on the 12 October 1992 Dahshour, Egypt, Earthquake, U.S. Geological Survey, Open-File Report 93-181.